Collector Efficiency Curves considering an Adapted Calculation Approach for Convective Heat Transfer in Insulating Gas Layers of Solar Collectors

Pascal Leibbrandt[1], Federico Giovannetti[2], Thomas Schabbach[1], Ulrike Jordan[3]

[1] Hochschule Nordhausen, Institute for Renewable Energy Technology (in.RET), Weinberghof 4, Nordhausen (Germany)

[2] Institute for Solar Energy Research Hamelin (ISFH), Am Ohrberg 1, Emmerthal (Germany)

[3] Kassel University, Institute of Thermal Engineering, Kassel (Germany)

Abstract

Recent investigations of the heat transfer in a gas layer between parallel plates heated from below indicate that there is a convective flow also below the critical Rayleigh number of 1708 in the so-called conductive flow regime. Based on experimental investigations, a correction term is proposed in this study that better characterizes the heat transfer below the critical Rayleigh number. The aspect ratio of the insulating gas layer is identified as the dependent variable of the correction function, which has a significant influence on the flow regimes and thus the heat transport phenomena that occur. This paper presents collector efficiency curves of a glass collector. Taking into account the convective flow at the critical Rayleigh number, the Nusselt number is increased by about 23 % for an aspect ratio of 48. This leads to an increase of the collector efficiency by nearly 3 % for a temperature difference of 40 K between the collector fluid and ambient temperature, and more than 6 % for a temperature difference of 60 K.

Keywords: heat transfer, convective heat transfer, conductive / postconductive regime, insulating glass, insulating gas layers, solar collector, calculation approach

1. Introduction

Aim of the presented investigation is to determine the heat transfer in inclined insulation gas layers, heated from below. The heat transfer in inclined gas layers is particularly important for standard flat-plate solar collectors as well as for novel insulating glass solar collectors.

The transition point between conductive and convective heat transfer in inclined gas layers, characterized by the critical Rayleigh number Ra_{crit}, was already studied analytically and experimentally from the 1960s and following years. All known investigations assume pure conduction below the critical Rayleigh number, whereas already Hollands et al. (1976) describe a flow with deflections at the lower and upper end of the gas layer.

However, measurements on solar flat-plate and insulating glass collectors show that heat losses are significantly higher than expected on the basis of pure heat conduction. For example, Bartelsen et al. (1993) and Föste (2013) showed deviations of up to 32 % between experimental and numerical data.

Also, previous investigations with computational fluid dynamics (CFD) simulations show that the assumption of pure heat conduction up to Ra_{crit} is only valid for very large aspect ratios. The aspect ratio $AR_{20} = L_{20}/s_{20}$, as shown in Fig. 1, describes the ratio of the length L_{20} of the gas layer and its thickness s_{20}.

This paper presents experimental investigations of insulating glazing with different geometries and aspect ratios in the subcritical Rayleigh number regime. Further details can be found in Leibbrandt et al. (2022).

doi:10.18086/eurosun.2022.12.08 Available at http://proceedings.ises.org

2. Heat Transfer in Enclosed Insulating Gas Layers Heated from Below

Fig. 1 shows a scheme of the investigated setup, consisting of two parallel, plane glass panes (10) and (30) with a space in between filled with argon (20). The lower glass pane (30) is heated from below to induce a uniform temperature field $T_{31}(x,y)$. The aim of the investigations presented here is to determine the convective heat transfer coefficient $h_{20,c}$ in the gas layer between surfaces (13) and (31) at temperatures $T_{13} < T_{31}$, see Fig. 1.

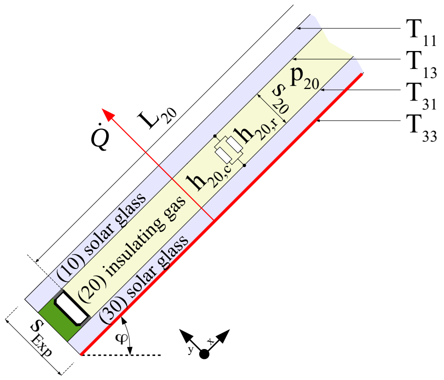

Fig. 1: Geometry and boundary conditions of the setup

The heat transfer $\dot{Q}$ between the two glass panes is determined by internal free convection and radiation. The heat transfer rate is

$$\dot{Q} = A_{20} \cdot h_{20} \cdot (T_{31} - T_{13}) \tag{1}$$

with the area $A_{20} = L_{20} \cdot B_{20}$ and the gas layer width B_{20}. The total heat transfer coefficient h_{20} is the sum of the convective heat transfer coefficient $h_{20,c}$ and the radiative heat transfer coefficient $h_{20,r}$:

$$h_{20} = h_{20,c} + h_{20,r}. \tag{2}$$

The convective heat transfer coefficient $h_{20,c}$ is calculated from the Nusselt number Nu, which is specified for free convection as a function of the Rayleigh number Ra,

$$Nu = Nu(Ra). \tag{3}$$

The Rayleigh number is the product of the Grashof number Gr, which relates the buoyancy forces to the internal viscous friction forces, and material properties, expressed by the Prandtl number Pr.

Hollands et al. (1976) developed the following Equation 4 from experimental investigations. The Equation 4 is a function of the Rayleigh number and it is divided into three parts. The operator $[...]^+ = (|[...]| + [...])/2$ elicits that only positive values of the argument are used, i.e. it eliminates the term if the argument is negative. $Ra^* = Ra \cdot \cos(\varphi)$ is also called modified Rayleigh number, where φ as the inclination angle, see Fig. 1.

$$Nu = 1 + 1.44 \cdot A \cdot [B]^+ + [C]^+ \tag{4}$$

with:

$$A = 1 - \frac{1708 \cdot (\sin(1.8 \cdot \varphi))^{\frac{1}{6}}}{Ra \cdot \cos(\varphi)} \qquad B = 1 - \frac{1708}{Ra \cdot \cos(\varphi)} \qquad C = \left(\frac{Ra \cdot \cos(\varphi)}{5830}\right)^{\frac{1}{3}} - 1$$

The heat transfer is characterized by three flow regimes:

- At lower Rayleigh numbers ($Ra^* < 1708$) the conductive behavior dominates, since the flow velocities are very small. This flow regime is called **conductive regime.**
- With increasing Rayleigh numbers ($1708 < Ra^* < 5830$) the flow velocity increases and a monocellular basic flow develops. In this range of Rayleigh numbers, the regime is called **immediate postconductive regime.**

- With an even higher Rayleigh number ($Ra^* > 5830$) the monocellular flow decays into a multicellular flow with several convection rolls. This flow type is called **high Rayleigh number regime.**

The lowest heat transfer through the gas layer and thus the highest solar collector efficiency is reached for the distance $s_{20,opt}$, that corresponds to a modified Rayleigh number of $Ra^* = 1708$. For $Ra^* = 1708$ the convective heat transfer is at its minimum.

Preliminary 2D and 3D CFD simulations presented in Leibbrandt et al. (2018) found that the aspect ratio AR is an additional influencing parameter for the convective heat transfer coefficient in the gas layer for the same reference conditions as used in the experimental setup by Hollands et al. (1976).

3. Experimental Investigations on Insulating Glazing

The heat transfer through three different insulating glazings is measured in a guarded hot box according to EN 12664 (2001) specifically conceived for measurements at temperatures up to 90 $°C$ and variable tilted angles, see Fig. 2(a). The insulating glazings, Fig. 2(b), have the basic dimensions of 500 mm x 500 mm. The length of the gas layer is $L_{Exp} = 480$ mm. The layer thicknesses s_{20} varied between 10, 8 and 6 mm. It can be adjusted by using different spacers. The resulting aspect ratios are $AR_{Exp} = 48$, 60 and 80, respectively.

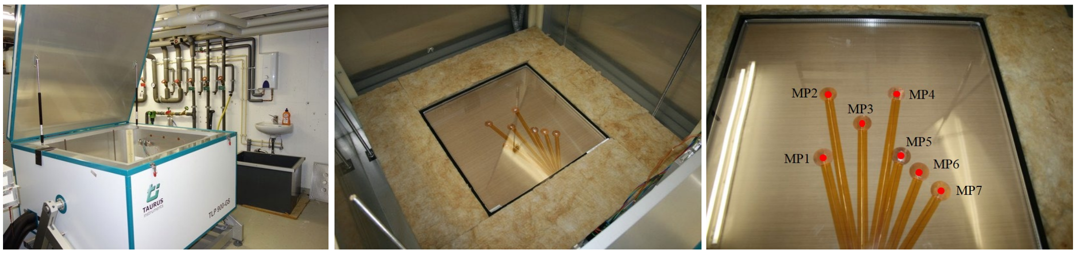

Fig. 2: 2(a) Pictoral view of the test facility, 2(b) View of the insulating glazing in the test facility, 2(c) Detailed view of the temperature sensors position on the insulating glazing

The temperature difference $\Delta T_{Exp} = T_{33} - T_{11}$ between the surfaces of the insulating glazing is measured with temperature sensors on the outer surfaces of the insulating glazing at the measuring points MP1 - MP7 on both sides of the insulating glazing, see Fig 2(c). The thermal resistance and the resulting equivalent thermal conductivity k_{Exp} (with the approach $\dot{q}_{Exp} = k_{Exp}/s_{Exp} \cdot \Delta T_{Exp}$) are determined from the measured values.

As boundary conditions for the experiment, the insulating glazing mean temperatures $T_{Exp} = 20$, 40, 60 and 80 $°C$ at $\Delta T_{Exp} \approx 20$ K are set ($T_{Exp} = (T_{11} + T_{33})/2$). For each specimen of insulating glazing, the measurement is carried out for tilt angles of 0, 20, 40 and 60°.

With the measured heat flow rate $\dot{q}_{Exp}$ and the measured temperature difference ΔT_{Exp} between the surfaces of the insulating glass, the total thermal resistance of the probe R_{Exp} can be determined. The total resistance R_{Exp} is the sum of the serial resistances of the glass panes $R_{Exp,10}$ and $R_{Exp,30}$ (with k_{Gl} and s_{Gl}) and the resistance of the insulating gas $R_{Exp,20}$:

$$R_{Exp} = R_{Exp,10} + R_{Exp,20} + R_{Exp,30} \tag{5}$$

The resistance of the gas layer $R_{Exp,20}$ results from the parallel resistances for free convection $R_{Exp,20,c}$ and radiation $R_{Exp,20,r}$:

$$\frac{1}{R_{Exp,20}} = \frac{1}{R_{Exp,20,c}} + \frac{1}{R_{Exp,20,r}} \tag{6}$$

With the definition $R_i = 1/(h_i \cdot A)$ and $A =$ const., Equation 5 in combination with Equation 6 gives the determining Equation for the convective heat transfer coefficient.

$$h_{Exp,20} = h_{Exp,20,c} + h_{Exp,20,r} \tag{7}$$

The radiative heat transfer coefficient $h_{Exp,20,r}$ in Equation 7 is calculated with an emission coefficient of $\epsilon_{Gl} = 83.7$ % for the uncoated float glass panes. The Nusselt numbers Nu_{20} for the experimental data are determined according to the definition in Equation 8

$$Nu_{20} = h_{Exp,20,c} \cdot \frac{s_{20}}{k_{20}} \tag{8}$$

with the experimentally determined convective heat transfer coefficient $h_{Exp,20,c}$, the gas layer thickness s_{20} and the temperature-dependent gas conductivity k_{20}.

Fig 3 shows the Nu_{20} numbers determined from the measurements as a function of the modified Ra* number. For horizontal plates and Ra* just above Ra^*_{crit}, the convective heat transfer coefficient exceeds the purely conductive one by more than 30 % ($Nu_{20} = 1.33$); for Ra* around 2400, Nu_{20} is already very close to the value given by Equation 4, with $Nu_{20}/Nu_{Holl} = 1.02$.

A measurement error analysis of all influencing variables with errors occurring during the measurement and a measurement error propagation results in a maximum uncertainty with respect to the experimentally determined Nusselt number Nu_{20} of ± 12.9 %. Details of the measurement error analysis and supplementary figures with error bars can also be found in Leibbrandt et al. (2022).

4. Recommended Relationship for the Nusselt Number below Ra_{crit}

The investigations show, that also below the critical Rayleigh number Ra^*_{crit} there is a convective heat transfer in the gas layer. To describe the Nusselt number Nu_{20} for $Ra^* < 1708$, a correlation is proposed as a quadratic function of the aspect ratio for $48 \leq AR \leq 80$. It is derived from mean values of the Nu_{20} values for each aspect ratio. The resulting correlation is given in Equation 9:

$$D = \frac{Nu_{20}}{Nu_{Holl}} = D_2 \cdot AR^2 + D_1 \cdot AR + D_0 \tag{9}$$

with:

$D_2 = 1.292 \cdot 10^{-4}$, $D_1 = -2.283 \cdot 10^{-2}$ and $D_0 = 2.035$

The correlation corrects the previous assumption of pure conduction for $Ra^* < 1708$ in Equation 4, validated for $48 \leq AR \leq 80$. Combining Equation 4 and 9 results in Equation 10:

$$Nu = max \begin{cases} D \\ 1 + 1.44 \cdot A \cdot [B]^+ + [C]^+ \end{cases} \tag{10}$$

The proposed correction to the Nusselt number describes convective heat transfer for small aspect ratios below the critical Rayleigh number. For an aspect ratio of 48, the relation yields a Nusselt number of about 1.23. Fig 3 indicates the impact of Equation 10 on the Nusselt number compared to the Hollands et al. (1976) approach for $48 \leq AR \leq 80$.

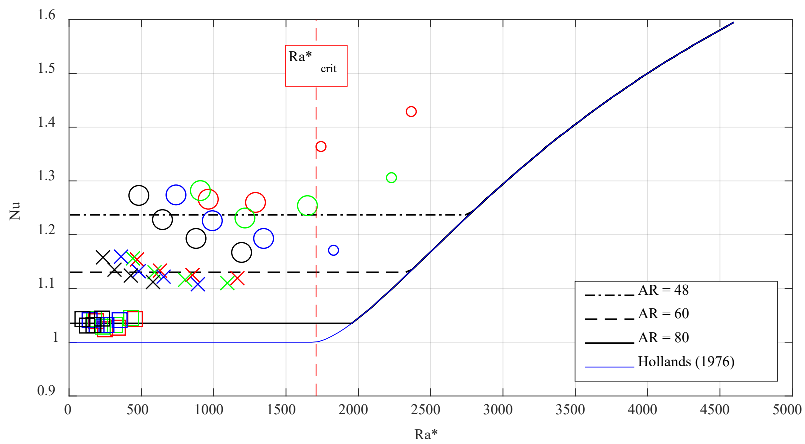

Fig. 3: Experimentally determined data (symbols) and their mean values (black lines) in comparison to the approach according to Hollands et al. (1976) (blue line). AR = 48 (O), AR = 60 (X) and AR = 80 (□), red for $\varphi = 0°$, green for $\varphi = 20°$, blue for $\varphi = 40°$, and black for $\varphi = 60°$ with $Ra^* = Ra \cdot \cos(\varphi)$. Measurement data above $Ra^* = 1708$ are not accounted for the correction (small symbols).

5. Effect on collector efficiency

A collector model is used to investigate the influence of the heat transfer coefficient $h_{20,c}$ modified with the correction function on the collector efficiency of an insulating glass collector according to Leibbrandt et al. (2018).

The thermal collector model is developed as part of a research project and is described in Schabbach et al. (2018). In a thermal network with 34 temperature nodes, each node represents one isothermal subsurface of a component or an isothermal volume. A temperature difference between two nodes leads to a heat flow whose magnitude depends on the temperature difference as well as the thermal resistance between the nodes. All types of heat transfer, occurring in the solar collector, are considered in the thermal network (conduction, natural and forced convection and thermal radiation). The multidimensional thermal network is verified only in terms of the individual heat transfer resistances and the associated heat flows. It could not be validated by measurements due to problems in manufacturing the insulating glass collector. However, the method used for thermal modeling based on temperature nodes is validated on the example of standard flat-plate collectors with collector measurements. The thermal model is used here only for estimating influencing parameters on collector heat losses and collector performance.

Fig. 4 shows the influence of the heat transfer coefficient $h_{20,c}$ on the collector efficiency η. As shown in Fig. 3, the experimentally determined Nusselt number below the critical Rayleigh number is at maximum 1.3, which also increases the value of the heat transfer coefficient in the range of about 30 %, so it is $h'_{20,c} = 1.3 \cdot h_{20,c}$. The effects on the collector characteristics for an increase of the heat transfer coefficient $h_{20,c}$ by 10 % - 30 % are shown in Fig. 4.

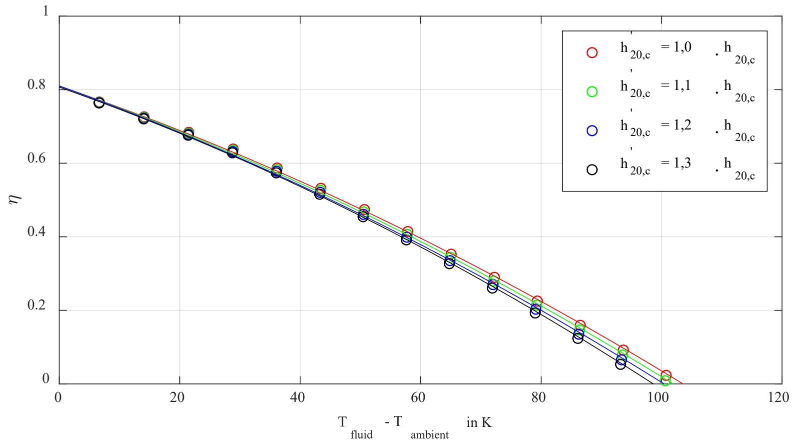

Fig. 4: Collector characteristics based on the thermal collector model with adapted heat transfer coefficients

For an increase of the heat transfer coefficient $h_{20,c}$ by 30 % and a temperature difference between the collector fluid and the ambient air of 40 K the collector efficiency η decreases by 2.7 % if the convective heat transfer in the so-called conductive flow regime is taken into account by the correction term as described in Equation 10.

If the temperature difference T_{fluid} - $T_{ambient}$ increases to 60 K, the deviation of the collector efficiency from the standard model due to the convection heat transfer, increases to about 6.4 %. Thus, the heat transfer correction is significant especially for high temperature differences.

This results in a reduction of the stagnation temperature ($\eta \rightarrow 0$) by about 5 to 6 K.

6. Conclusion

Experiments of an enclosed gas layer between two glass panes show that the heat transfer below the critical Rayleigh number Ra_{crit} is higher than the conductive heat transfer assumed so far. The investigations show that there is a convective share of the heat transfer in the gas layer also below the critical Rayleigh number.

For small aspect ratios (here 48), there is an increase of the heat transfer compared to pure conductive regime by 23 % for the examined conditions.

To describe this convective heat transfer, a novel relationship is proposed for the Nusselt number as a function of the aspect ratio, but not a dependence of the inclination angle in the subcritical regime. In particular, the transition near and above the critical Rayleigh number should be examined in detail with further experimental investigations to improve the presented results.

For a temperature difference between fluid an ambient of 60 K, the deviation of the collector efficiency from the standard model due to the convection heat transfer, increases to about 6.4 %, calculated with a thermal collector model.

References

Bartelsen, B., Jansen, S., Rockendorf, G., 1993. Heat Transfer by Natural Convection in the Air Gap of Flat Plate Collectors. Proceedings ISES Solar World Congress, pp. 267-273, Budapest, Ungarn

Föste, S., 2013. Flachkollektor mit selektiv beschichteter Zweischeibenverglasung. Dissertation, Gottfried Wilhelm Leibniz Universität Hannover

Hollands, K.G.T., Unny, T.E., Raithby, G.D., Konicek, L., 1976. Free Convective Heat Transfer Across Inclined Air Layers. J. Heat Transfer 98(2), 189-193

Leibbrandt, P., Schabbach, T., Dölz, M., Rhein, M., 2018. Untersuchungsergebnisse zur Strömung und Wärmeübertragung im Nurglaskollektor. 28. OTTI Symposium Thermische Solarenergie, Bad Staffelstein

Leibbrandt, P., Giovannetti, F., Schabbach, T., Jordan, U., 2022. Improved calculation approach of the heat transfer in inclined insulating gas layers. Solar Energy. Volume 231, January 2022, Pages 252-261

Schabbach, T., Leibbrandt, P., 2018. Abschlussbericht zum Vorhaben NUGLACOL – Nurglas-Solarflachkollektor. Entwicklung eines kostengünstigeren solaren Flachkollektorsystems auf Glas-Basis. Kurzbezeichnung: NuGlaCol. Förderkennzeichen: 0325557A. Laufzeit: 01.03.2015 - 31.05.2018. Nordhausen

Thermal performance of building materials and products - Determination of thermal resistance by means of guarded hot plate and heat flow meter methods - Dry and moist products with medium and low thermal resistance; German version EN 12664:2001